Influence of local electron interactions on phonon spectrum in iron

Jan Łażewski,[1,*] Przemysław Piekarz,[1] Andrzej M. Oleś,[1,2] and Krzysztof Parlinski[1]
[1]*Institute of Nuclear Physics, Polish Academy of Sciences, Radzikowskiego 152, PL-31342 Kraków, Poland*
[2]*Max-Planck-Institut für Festkörperforschung, Heisenbergstrasse 1, D-70569 Stuttgart, Germany*
(Received 1 September 2006; published 27 November 2006)

The density functional generalized-gradient approximation with the local Coulomb interaction U and the direct method have been applied to study the electronic structure and the phonon spectrum of Fe α bcc phase. The electronic structure, the equilibrium lattice constant, as well as phonon frequencies and phonon density of states are found to depend primarily on the interaction between the electrons of equal spin $U-J$, where J is Hund's exchange element. We have found that the results of the present *ab initio* calculations reproduce quite well the phonon density of states obtained from inelastic neutron scattering for $U \simeq 1.0$ eV and $J \simeq 0.5$ eV, suggesting a considerable screening of local Coulomb interactions in iron.

DOI: 10.1103/PhysRevB.74.174304 PACS number(s): 63.20.Dj, 71.20.Be, 75.50.Bb, 75.80.+q

I. INTRODUCTION

The origin of ferromagnetism in itinerant systems remains one of the open questions in the condensed matter theory. It is quite remarkable that density functional theory (DFT) gives correctly several predictions concerning the stability of ferromagnetism and the values of magnetic moments in ordered phases.[1] This standard approach to the description of ferromagnetism in itinerant system was proposed originally by Stoner, and next refined within the modern methods of calculating the electronic structure, both in the *ab initio* approach[2] and in parametrized tight-binding methods.[3] This basically one-electron theory has been tested in numerous density functional and model calculations. Although important corrections which go beyond this approach follow from local electron correlations,[4] the local density approximation (LDA) is frequently quite successful when appropriate correction terms are included. For instance, in the case of Fe, preliminary studies within the LDA predicted incorrect ground state crystal symmetry with nonmagnetic state.[5] However, when gradient corrections were included in the potential, the experimentally observed bcc structure and ferromagnetic state were obtained.[6] Further studies, performed within the generalized gradient approximation (GGA) confirmed that the electronic structure and magnetic moments are well reproduced within the one-electron electronic structure calculations.[7,8] These remarkable successes were possible as the errors in the treatment of electron correlations within the LDA compensate each other to a large extent.[9]

Despite these successes, there are still many aspects of magnetism in transition metals that are not well understood. One of the open questions concerns the role of short-range Coulomb interactions and their effect on the electronic structure.[10] These local interactions lead to correlation effects[4] among $3d$ electrons in the partially filled $3d$ states which form narrow bands, in contrast to more extended $4s$ and $4p$ states, where such local correlation effects are negligible. The on-site Coulomb interactions between electrons in $3d$ states are usually parametrized by the Hubbard repulsion energy U and Hund's exchange element J.[11] A proper treatment of correlation effects requires theoretical methods which go beyond the one-electron approach, such as the dynamical mean field theory (DMFT). In the lowest order, however, the effect of U on the electronic structure is frequently studied in the Hartree-Fock approximation, which leads to so-called LDA+U method[12] (or GGA+U) when implemented in the DFT framework.

Although the importance of electron correlations has been realized for many years, the determination of an accurate value of U for a given transition metal remains a formidable task.[13] Complex multiband screening and intersite interactions strongly influence U and change its effective value.[14] The values obtained from the constraint DFT are largely overestimated (3–5 eV) and lead to unphysical features in the electronic structure.[13] On the contrary, the empirical methods[3] are very successful when much lower values $U \sim 1-2$ eV are used. For instance, taking $U=1$ eV one gets the best agreement between calculated and experimental photoemission spectrum.[15] Including finite U leads to qualitative improvement of the magnetic anisotropy in Fe and Ni, and good agreement with experiment was achieved for $U=1.2$ eV.[16] Even by considering the electron correlation effects beyond the Hartree-Fock, one finds relatively low $U \sim 2$ eV in iron,[4] which may be considered as an upper limit. All these results have shown that the studies of correlation effects in transition metals are more subtle than in transition metal oxides, where $3d$ electrons localize, the screening within the $3d$ subsystem is absent, and the values of U are much larger.

Under these circumstances any information concerning the dependence of physical properties of iron on the actual Coulomb interaction is very valuable and might help to establish the realistic value of U for this transition metal. In the present contribution we focus on lattice dynamics that is known to depend on magnetic properties.[17] A good example is ferromagnetic metal $SrRuO_3$, where strong spin-phonon interaction leads to anomalous behavior of Raman modes at T_c.[18] The theory of electron-phonon coupling in ferromagnetic metals, developed by Kim,[19] predicts the spin-dependent screening effect on phonon frequencies. Indeed, the *ab initio* studies of Ni confirmed that phonon dispersions are significantly influenced due to magnetically modified screening.[17] On the contrary, the changes in phonon spectrum induced by local Coulomb interactions and the accompanying changes of short-range spin correlations in metallic materials are not well understood until now. One of the most spectacular results was obtained recently for plutonium by means of the DMFT, showing that electron correlations in $5f$

states strongly influence the phonon spectrum.[20] Local Coulomb interactions change significantly phonon frequencies also in $PuCoGa_5$ superconductor, as shown by a recent study implementing these interactions within the GGA+U method.[21] In fact, this dependence of the phonon spectra on U is of importance for a quantitative comparison with experimental data.[22]

Phonon spectrum of iron was studied within the density functional approach by the linear-response[23,24] and small displacement methods.[25] It was demonstrated that the GGA gives a better agreement with the inelastic neutron scattering measurements than the LDA.[23] In this paper we study the effect of local Coulomb interaction U on lattice dynamics in Fe using the GGA+U method. By comparing with the experimental phonon frequencies, we could find an upper bound for the value of effective U. Thus, our approach provides a complementary way of estimating the Coulomb interaction in transition metals to that available from purely electronic studies which focus on the exchange splitting and magnetic moment.

The paper is organized as follows. In Sec. II we describe the method of calculation and present the electronic structure of Fe as a function of U. The role of the proper choice of Hund's exchange J which is able to reproduce the experimental magnetic moment in the ferromagnetic ground state of iron is also discussed. In Sec. III we focus on the phonon dispersion curves and phonon density of states, and their dependence on the parameters which describe Coulomb interactions. Discussion and conclusions are presented in Sec. IV.

II. CALCULATION METHOD AND GROUND STATE PROPERTIES

For the determination of the electronic structure of iron we have used the GGA approach,[26] implemented in the VASP program.[27] The calculations were carried out in the $3\times3\times3$ supercell containing 54 atoms within the bcc $Im\bar{3}m$ space-group symmetry constraints. Eight valence electrons for each atom were represented by plane waves with the energy cutoff $E_{\mathrm{cut}}=350$ eV (the contributions due to higher energies are negligible). The wave functions in the core region were evaluated using the full-potential projector augmented-wave (PAW) method.[28] The summation in the reciprocal space were performed on the $8\times8\times8$ **k** grid with 35 irreducible points in the used $3\times3\times3$ cell, i.e., $24\times24\times24$ **k** grid per one crystallographic unit cell, generated by the Monkhorst-Pack scheme.[29]

The local Coulomb interactions between $3d$ electrons are approximately described by two parameters:[11] the intraorbital Coulomb repulsion U and interorbital Hund's exchange J. In the present study we apply the implementation of electron interactions adapted in VASP program,[27] which uses the following approximate expression:

$$H_{\mathrm{int}} = U\sum_{i\alpha} n_{i\alpha\uparrow}n_{i\alpha\downarrow} + \left(U-\frac{1}{2}J\right)\sum_{i,\alpha<\beta} n_{i\alpha}n_{i\beta} + J\sum_{i,\alpha<\beta}\left(d^{\dagger}_{i\alpha\uparrow}d^{\dagger}_{i\alpha\downarrow}d_{i\beta\downarrow}d_{i\beta\uparrow} + d^{\dagger}_{i\beta\uparrow}d^{\dagger}_{i\beta\downarrow}d_{i\alpha\downarrow}d_{i\alpha\uparrow}\right) - 2J\sum_{i,\alpha<\beta}\mathbf{S}_{i\alpha}\cdot\mathbf{S}_{i\beta}. \quad (1)$$

Here $d^{\dagger}_{i\alpha\sigma}$ are the electron creation operators in $3d$ states for the orbital state α and spin state $\sigma=\uparrow,\downarrow$ at site i, $n_{i\alpha}=\Sigma_{\sigma}n_{i\alpha\sigma}$ is the electron density operator, and $\mathbf{S}_{i\alpha}=\{S^{x}_{i\alpha},S^{y}_{i\alpha},S^{z}_{i\alpha}\}$ is the spin operator for the orbital state α at site i. This form of interaction is only approximate, as the complete Coulomb interactions are anisotropic and satisfy certain constraints due to the *rotational invariance* in the orbital space.[11] In the Hartree-Fock approximation which is next used to generate the one-particle potentials for $\{\alpha\sigma\}$ spin orbitals only the diagonal terms contribute, so one may write,

$$H_{\mathrm{int}} \simeq U\sum_{i\alpha} n_{i\alpha\uparrow}n_{i\alpha\downarrow} + U\sum_{i,\alpha<\beta,\sigma} n_{i\alpha\sigma}n_{i\beta\bar{\sigma}} + (U-J)\sum_{i,\alpha<\beta,\sigma} n_{i\alpha\sigma}n_{i\beta\sigma} \quad (2)$$

with $\bar{\sigma}=-\sigma$. We adopted the standard Hartree-Fock potentials which result from these interactions within the LDA+U method.[12] Note that the value of U is then an average value which stands for the Coulomb repulsion between two electrons of opposite spins, either in different orbitals or in the same orbital. The effective Coulomb interaction between two electrons of the same spin is given by

$$U_{\mathrm{eff}} = U - J, \quad (3)$$

i.e., is reduced by Hund's exchange element.

For each parameter set we performed the minimization of the total energy of the crystal, and found the optimized lattice constant a and the corresponding electronic structure. In Table I we compare the lattice parameters and magnetic moments obtained for representative values of the electronic interactions U and J with the experimental data. For $U=J=0$ the lattice constant a is underestimated by about 1.4%. Increasing U enhances both the magnetic moment and the lattice constant, so it leads to better agreement with the experimental value of a. However, the magnetic moment is well reproduced already for $U=J=0$, and is slightly larger for $U=1.0$ eV, $J=0.5$ eV, while it is close to saturation and significantly overestimated both for $U=1.0$ eV, $J=0$ and for $U=2.0$ eV, $J=0.8$ eV (by about 18%).

The electronic density of states (DOS) $N(E)$, plotted for up-spin and down-spin subbands separately, is shown in Fig. 1. While the total spectral weight at the Fermi energy (E_F) depends only very weakly on U, the main effect of local Coulomb interactions is the downward shift of the maximum in the majority (up-spin) $3d$ DOS located at ~-1 eV below E_F. At the same time, the corresponding maximum for the minority (down-spin) subband at ~2 eV above E_F moves to higher energies. As a result, the exchange splitting between up- and down-spin subbands increases. In fact, for $U=2$ eV, $J=0.8$ this shift is already much larger than observed experimentally.[15] In addition, there is a qualitative change of the spin character of the electronic density at E_F, from up to down spin.

The results shown in Table I suggest that the Coulomb interaction U plays a more important role in the magnetism of iron than the Hund's exchange J. This impression is however misleading and would contradict the usual scenario that

TABLE I. Lattice constant a, volume V and magnetic moment m of Fe, as obtained for different values of U and J. Experimental values are taken from Ref. 32.

U (eV)	J (eV)	a (Å)	V (Å^3)	m (μ_B)
0.0	0.0	2.83	22.67	2.22
1.0	0.0	2.88	23.81	2.62
1.0	0.5	2.84	22.89	2.28
1.0	0.8	2.83	22.69	2.17
2.0	0.8	2.88	22.88	2.63
Experiment		2.87	23.64	2.22

the magnetic instability in itinerant models which involve nearly degenerate 3d states follows from Hund's exchange interaction, which indeed determines the Stoner parameter $I \propto J$ in spin-polarized LDA methods.[30] However, the situation in the ferromagnetic states close to saturation of the magnetization is different. Here instead the interaction between the electrons of the same spin, see Eq. (3), plays an essential role and this interaction energy U_{eff}, is decreased when J increases. Therefore, for a fixed value of U the magnetization decreases with increasing J (see Fig. 2). In fact, this effect consists of the change induced by (i) the electronic interactions alone, and (ii) the change of the volume as the lattice constant decreases with increasing J [Fig. 2(b)]. Therefore, the overall dependence of m on J which follows from U_{eff} is even amplified by the increasing lattice constant a for the systems with large magnetic moments m, found in Fe for small values of J, as shown in Fig. 2(a).

III. PHONON DISPERSION CURVES

For crystal structures optimized with different U and J values, the phonon dispersion curves were calculated using the direct method.[31] First, the Hellmann-Feynman forces were obtained by making the displacements of Fe atoms from their equilibrium positions. Second, the force constant matrix was derived by the singular value decomposition method. Finally, the dynamic matrix was constructed and diagonalized for selected values of reciprocal space **k** vector. In the considered supercell the exact frequencies are calculated at Γ and H points. However, because of relatively large supercell size used in the calculations, all phonon frequencies were obtained with only rather small errors in the entire Brillouin zone. The measure of accuracy of phonon frequencies derived from the direct method is the highest neglected force constant which (in our case) is more than two orders of magnitude smaller than the strongest one considered in the presented systems. Under these circumstances, the errors in

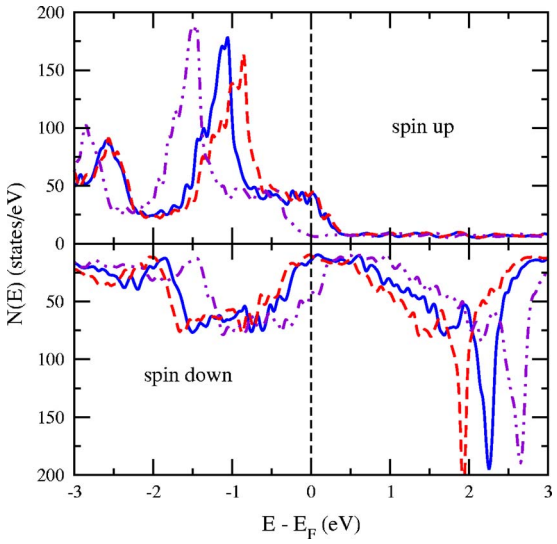

FIG. 1. (Color online) The electron density of states $N(E)$ for Fe, as obtained with $U=J=0$ (dashed line), $U=1.0$ eV and $J=0.5$ eV (solid line), and $U=2.0$ eV and $J=0.8$ eV (dashed-dotted line).

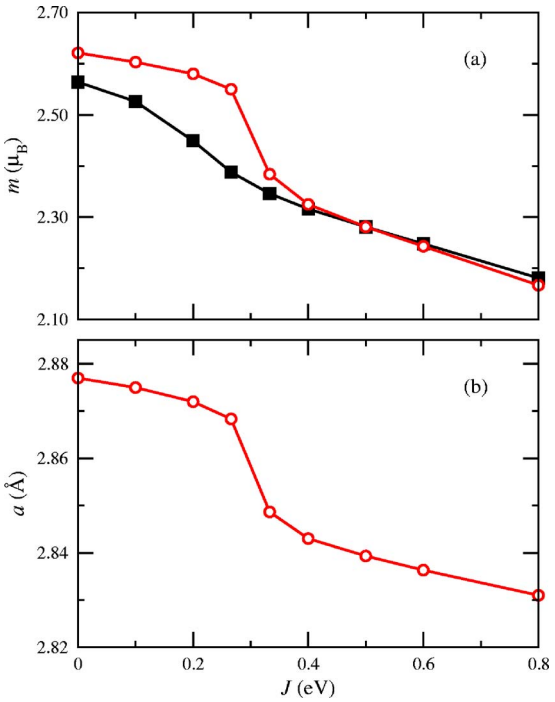

FIG. 2. (Color online) Properties of the Fe ground state found in the GGA+U method with $U=1.0$ eV for increasing J (empty circles): (a) magnetic moments m (in units of μ_B), and (b) lattice constant a (in units of Å). Filled squares in panel (a) show the magnetic moments obtained for a fixed lattice constant a with $U=1.0$ eV and $J=0.5$ eV.

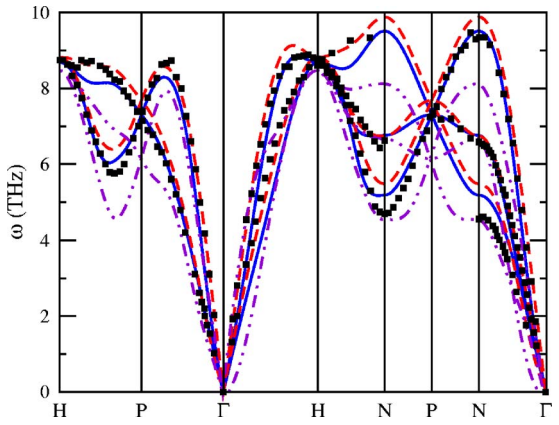

FIG. 3. (Color online) Phonon dispersion curves as obtained along high symmetry directions in the bcc Brillouin zone for $U=0$ (dashed lines), 1.0 eV (solid lines), and 2.0 eV (dashed-dotted lines). In all cases $J=0$. Experimental data (squares) are taken from Ref. 33. The high symmetry points are $H=\frac{2\pi}{a}(1,1,1)$, $P=\frac{2\pi}{a}(\frac{1}{2},\frac{1}{2},\frac{1}{2})$, $\Gamma=\frac{2\pi}{a}(0,0,0)$, $H=\frac{2\pi}{a}(0,0,1)$, $N=\frac{2\pi}{a}(\frac{1}{2},\frac{1}{2},1)$, $P=\frac{2\pi}{a}(\frac{1}{2},\frac{1}{2},\frac{1}{2})$, $N=\frac{2\pi}{a}(0,\frac{1}{2},\frac{1}{2})$, and $\Gamma=\frac{2\pi}{a}(0,0,0)$, where a is the bcc lattice constant.

the phonon frequencies could lead to practically invisible corrections in the data of Fig. 3.

The phonon dispersion curves along the high-symmetry directions are shown for $U=0$, $U=1.0$, and $U=2.0$ eV in Fig. 3. The experimental points were taken from inelastic neutron scattering experiment.[33] Generally, one finds that the difference between $U=0$ and $U=1.0$ eV is very small and in both cases the overall agreement with experiment is very good (within the accuracy of the method). A better agreement with $U=1.0$ eV is observed at the N point, where the lowest mode shows the largest discrepancy, but the data obtained with $U=0$ are closer to experiment for the highest phonon mode close to the H point. For $U=2.0$ eV, the calculated frequencies strongly soften, particularly near the Γ point, which leads already to large disagreement with the experimental points. This effect is particularly pronounced for the modes along the H-P and N-P directions.

We should note, however, that we have not taken into account the thermal effects when comparing the theoretical points (at $T=0$) with the inelastic scattering data obtained at room temperature. The increase in lattice constant due to thermal expansion and zero-point motion is about 0.3%.[23] This would reduce the highest phonon frequencies approximately by 4%. On the other hand, the obtained lattice constant $a=2.83$ Å is by 1.4% smaller than the experimental value. Therefore, a more accurate quantitative comparison of the theoretical and experimental data is not possible at the moment.

The influence of U on the phonon spectrum is even more pronounced in the phonon DOS (Fig. 4). One finds that already for $U=J=0$ the main features of the phonon DOS are correctly reconstructed. However, some peculiarities of the spectrum structure, especially about 5.5 and 8.7 THz, are better reproduced by the calculation with $U=1.0$ eV and $J=0.5$ eV. Looking at overall shape of the spectra, one can conclude that the positions of the two peaks as well as the

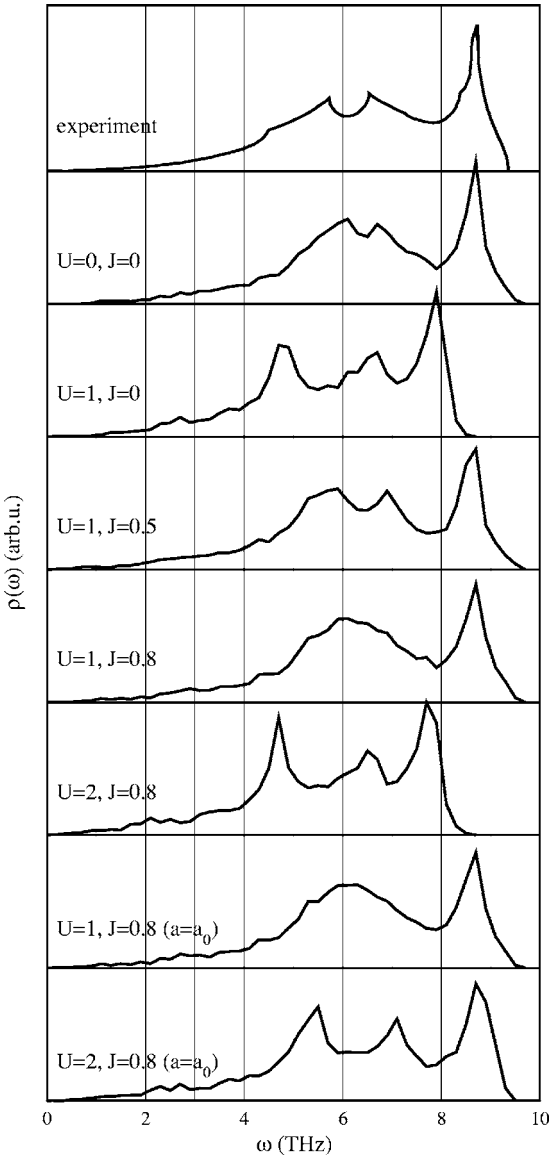

FIG. 4. A comparison of phonon density of states calculated for different values of U and J (both in eV) with that obtained from inelastic neutron scattering data for Fe (experiment) (Ref. 33). The two lowest curves were calculated with a fixed lattice constant $a=a_0$ obtained for $U=J=0$.

range of the phonon spectrum depend mainly on $U_{\text{eff}}=U-J$, rather than on U and J separately, in agreement with our observation concerning the magnetic moments m, made in the preceding section. Indeed, the spectrum calculated for $U=1.0$ eV, $J=0.8$ eV resembles that obtained with $U=J=0$, while the one for $U=2.0$ eV, $J=0.8$ eV that for $U=1.0$ eV, $J=0$ eV. As a general feature one finds that the phonon spectrum shifts monotonically to lower frequencies with increasing U_{eff}. This is associated with a direct dependence of phonon frequencies on lattice constant, which increases with U_{eff} [i.e., decreases with J, see Fig. 2(b)]. In fact, this effect is very similar to magnetostriction. Apart from overall softening, there are distinct qualitative changes induced by U. For instance, for $U=1.0$ eV and $J=0$, a large peak appears at ~5 THz, that is not observed in experiment.

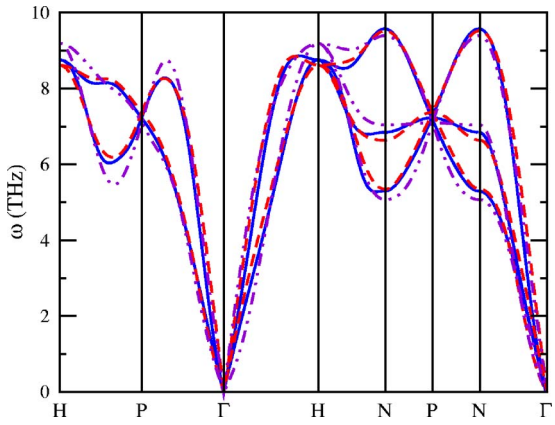

FIG. 5. (Color online) Phonon dispersion curves for Fe calculated with $U=J=0$ (dashed lines), $U=1.0$ eV, $J=0.5$ eV (solid lines), and $U=2.0$ eV, $J=0.8$ eV (dashed-dotted lines), with a fixed lattice constant $a=a_0$ obtained at $U=J=0$. High symmetry points as in Fig. 3.

To separate the influence originating from the expansion of lattice constant, we have repeated calculations of the lattice dynamics for $U=1.0$ eV, $J=0.8$ eV, and $U=2.0$ eV, $J=0.8$ eV with a constant value of $a=a_0$ obtained for $U=J=0$ (two bottom curves in Fig. 4). In this case one finds that the frequency range of the whole spectrum does not change significantly, whereas intensities and positions of individual peaks do. For $U=2$ eV, the phonon spectrum changes considerably at low energies, where transverse modes strongly soften and give a peak with large intensity at 5.5 THz. Interestingly, the highest frequencies at ~9 THz slightly increase. Similar behavior has been observed[21] also in the phonon spectrum of $PuCoGa_5$.

In order to clarify better the observed effects, we present in Fig. 5 phonon dispersion curves calculated for the same lattice constant with $U=J=0$, $U=1.0$, and $J=0.5$ eV, as well as for $U=2.0$ and $J=0.8$ eV. Apart from the transverse mode in Γ-H direction that softens near the Γ point, the most pronounced changes in phonon dispersions are seen at larger wave vectors $\mathbf{k}$. At the H point, the phonon energy increases by about 7%, and between H and P points, the transverse mode softens by 15% when the larger values of U and J are taken. These changes differ qualitatively from those discussed in Ref. 17, where the magnetization dependence of the phonon spectrum of Ni was studied. It was shown that the electron polarizability depends on magnetization only for small values of $\mathbf{k}$, and the strongest frequency shifts were observed close to the Γ point. Therefore, the frequency changes found here cannot be explained only by the enhanced magnetization, which depends on U and J rather weakly. These local interactions, however, strongly influence $3d$ electron states and charge density distribution, so in consequence interatomic screening and force constants are modified. Effectively, larger U leads to partial localization of $3d$ states, the electronic screening becomes weaker, and interatomic forces increase. This is clearly seen for some longitudinal modes, which harden with increasing U. A similar effect, however much more pronounced, is also observed in transition metal oxides, e.g., in the cuprates,[34] where insulator-metal transition induces strong softening of the bond-stretching mode at the Brillouin zone boundary.

IV. CONCLUSIONS

Summarizing, we have found that local Coulomb interactions significantly modify the phonons in iron. By putting together phonon DOS as well as phonon dispersion curves obtained for different values of U and J we found consistent changes of calculated spectra induced by increasing local Coulomb interaction. Therefore, the situation here is somewhat similar to that in $PuCoGa_5$,[21] but the electron interaction parameters $\{U,J\}$ are here smaller due to the itinerant character of $3d$ electrons in iron, in contrast to almost localized $5f$ electrons in $PuCoGa_5$. Although the measurement of phonon spectra in principle enables the estimation of these interaction parameters from experiment, accurate values of Coulomb repulsion U and Hund's exchange J components cannot be separately determined from such a comparison with experimental data. Nevertheless, present study allows one for a good estimation of U_{eff}. For $U_{\mathrm{eff}}=0.5$ eV one finds satisfactory agreement with the experiment both for the phonon DOS and for the magnetic moment, whereas $U_{\mathrm{eff}} \sim 1.0$ eV gives too soft phonon spectra, and an almost saturated magnetic moment, both features contradicting the experimental data. It implies that local Coulomb interactions $\{U,J\}$, which potentially induce strong changes in the phonon spectrum, are significantly screened by the itinerant electrons. We suggest that the values $U \simeq 1.0$ eV and $J \simeq 0.5$ eV deduced from the phonon spectra should be treated as an upper bound for the parameters of local Coulomb interaction in iron. In fact, such values are also used in the tight-binding methods.[3]

We have discussed two mechanisms responsible for the observed changes in phonon spectra. First, the increase in the local Coulomb repulsion increases lattice constant, and consequently leads to smaller phonon frequencies. Second, the modification of the $3d$ states induces changes in electronic polarizability and screening. With increasing U, the electronic states become more localized, and the effective screening decreases. We have shown that screening effects are stronger for larger $\mathbf{k}$ vectors, and this may be attributed to the local nature of Coulomb interaction U.

ACKNOWLEDGMENTS

This work was partially supported by the Polish Ministry of Science and Education under Contract No. 1 P03B 104 26. Calculations have been partially performed at the Academic Computational Center Cyfronet AGH, computational Grant No. MNiSW/SGI2800/IFJ/129/2006.

*Electronic address: jan.lazewski@ifj.edu.pl

[1] V. L. Moruzzi, J. F. Janak, and A. R. Williams, *Calculated Electronic Properties of Metals* (Pergamon, New York, 1978); J. Callaway and C. S. Wang, Phys. Rev. B **16**, 2095 (1977).
[2] H. C. Herper, E. Hoffmann, and P. Entel, Phys. Rev. B **60**, 3839 (1999).
[3] C. Barreteau, M. C. Desjonquères, A. M. Oleś, and D. Spanjaard, Phys. Rev. B **69**, 064432 (2004); G. Autès, C. Barreteau, D. Spanjaard, and M. C. Desjonquères, J. Phys.: Condens. Matter **18**, 6785 (2006).
[4] G. Stollhoff and P. Thalmeier, Z. Phys. B: Condens. Matter **43**, 13 (1981); A. M. Oleś and G. Stollhoff, Phys. Rev. B **29**, 314 (1984); G. Stollhoff, A. M. Oleś, and V. Heine, *ibid.* **41**, 7028 (1990).
[5] C. S. Wang, B. M. Klein, and H. Krakauer, Phys. Rev. Lett. **54**, 1852 (1985).
[6] P. Bagno, O. Jepsen, and O. Gunnarsson, Phys. Rev. B **40**, 1997 (1989).
[7] L. Stixrude, R. E. Cohen, and D. J. Singh, Phys. Rev. B **50**, 6442 (1994).
[8] E. G. Moroni, G. Kresse, J. Hafner, and J. Furthmüller, Phys. Rev. B **56**, 15629 (1997).
[9] G. Stollhoff, A. M. Oleś, and V. Heine, Phys. Rev. Lett. **76**, 855 (1996).
[10] M. I. Katsenelson and A. I. Lichtenstein, J. Phys.: Condens. Matter **11**, 1037 (1999).
[11] A. M. Oleś, Phys. Rev. B **28**, 327 (1983); A. M. Oleś, G. Khaliullin, P. Horsch, and L. F. Feiner, *ibid.* **72**, 214431 (2005).
[12] V. I. Anisimov, J. Zaanen, and O. K. Andersen, Phys. Rev. B **44**, 943 (1991); A. I. Liechtenstein, V. I. Anisimov, and J. Zaanen, *ibid.* **52**, R5467 (1995).
[13] M. M. Steiner, R. C. Albers, and L. J. Sham, Phys. Rev. B **45**, 13272 (1992).
[14] V. I. Anisimov and O. Gunnarsson, Phys. Rev. B **43**, 7570 (1991).
[15] R. E. Kirby, E. Kister, F. K. King, and E. L. Garwin, Solid State Commun. **56**, 425 (1985).
[16] I. Yang, S. Y. Savrasov, and G. Kotliar, Phys. Rev. Lett. **87**, 216405 (2001).
[17] J.-H. Lee, Y.-C. Hsue, and A. J. Freeman, Phys. Rev. B **73**, 172405 (2006).
[18] D. Kirillov, Y. Suzuki, L. Antognazza, K. Char, I. Bozovic, and T. H. Geballe, Phys. Rev. B **51**, 12825 (1995); M. N. Iliev, A. P. Litvinchuk, H.-G. Lee, C. L. Chen, M. L. Dezaneti, C. W. Chu, V. G. Ivanov, M. V. Abrashev, and V. N. Popov, *ibid.* **59**, 364 (1999).
[19] D. J. Kim, Phys. Rev. B **25**, 6919 (1982).
[20] X. Dai, S. Y. Savrasov, G. Kotliar, A. Migliori, H. Ledbetter, and E. Abrahams, Science **300**, 953 (2003); J. Wong, M. Krisch, D. L. Farber, F. Occelli, A. J. Schwartz, T.-C. Chiang, M. Wall, C. Boro, and R. Xu, *ibid.* **301**, 1078 (2003).
[21] P. Piekarz, K. Parlinski, P. T. Jochym, A. M. Oleś, J. P. Sanchez, and J. Rebizant, Phys. Rev. B **72**, 014521 (2005).
[22] S. Raymond, P. Piekarz, J. P. Sanchez, J. Serrano, M. Krisch, B. Janousova, J. Rebizant, N. Metoki, K. Kaneko, P. T. Jochym, A. M. Oleś, and K. Parlinski, Phys. Rev. Lett. **96**, 237003 (2006).
[23] A. Dal Corso and S. de Gironcoli, Phys. Rev. B **62**, 273 (2000).
[24] X. Sha and R. E. Cohen, Phys. Rev. B **73**, 104303 (2006).
[25] D. Alfe, G. Kresse, and M. J. Gillan, Phys. Rev. B **61**, 132 (2000).
[26] J. P. Perdew, J. A. Chevary, S. H. Vosko, K. A. Jackson, M. R. Pederson, D. J. Singh, and C. Fiolhais, Phys. Rev. B **46**, 6671 (1992).
[27] G. Kresse and J. Furthmüller, Comput. Mater. Sci. **6**, 15 (1996); Phys. Rev. B **54**, 11169 (1996).
[28] P. E. Blöchl, Phys. Rev. B **50**, 17953 (1994); G. Kresse and D. Joubert, *ibid.* **59**, 1758 (1999).
[29] H. J. Monkhorst and J. D. Pack, Phys. Rev. B **13**, 5188 (1976).
[30] O. Gunnarsson, J. Phys. F: Met. Phys. **6**, 587 (1976).
[31] K. Parlinski, Z. Q. Li, and Y. Kawazoe, Phys. Rev. Lett. **78**, 4063 (1997); K. Parlinski, software PHONON, Cracow, 2004.
[32] *Magnetic Properties of Metals: d-Elements, Alloys and Compounds*, Data in Science and Technology, edited by H. P. J. Wijn (Springer, Berlin, 1991).
[33] C. Van Dijk and J. Bergsma, *Neutron Inelastic Scattering* (IAEA, Vienna, 1968), Vol. 1, p. 233.
[34] R. J. McQueeney, Y. Petrov, T. Egami, M. Yethiraj, G. Shirane, and Y. Endoh, Phys. Rev. Lett. **82**, 628 (1999).